Optical spectra of two-dimensional photonic crystal bars based on macroporous Si

Sergey A. Dyakov[a,c], Ekaterina V. Astrova[b], Tatiana S. Perova[a], Vladimir A. Tolmachev[b], Galina V. Fedulova[b], Anna Baldycheva[a], Viktor Yu. Timoshenko[c], Sergei G. Tikhodeev[d], Nikolay A. Gippius[d]

[a]Trinity College Dublin, Dublin 2, Ireland
[b]Ioffe Physical Technical Institute, RAS, St. Petersburg, 194021, Russia
[c]Faculty of Physics, Moscow University, Leninskie Gory 1, 119991, Moscow, Russia
[d]General Physics Institute, RAS, Vavilova 38, Moscow, 119991, Russia

ABSTRACT

Two-dimensional (2D) photonic crystal (PC) bars with 6 and 21 periods were fabricated by simultaneous photo-electrochemical etching of macropores and trenches in a pre-patterned silicon wafer. The structures had square lattice of cylindrical pores and were terminated by nonmodulated silicon pre-layers. The infrared reflection spectra of the PC bars have been simulated using scattering matrix method. In order to take into account the roughness of pore inner surface an additional silicon layer around the pores was introduced with a fitted complex refractive index. A comparison between the simulated refection spectra and those obtained experimentally demonstrates a satisfactory agreement in the region of secondary photonic band gaps.

Keywords: Photonic Crystals, Two-Dimensional Photonic Crystals, Scattering Matrix Method, FTIR Spectroscopy, Photonic Band Gaps

1. INTRODUCTION

Experimental investigations of optical properties of two-dimensional (2D) photonic crystals (PCs) based on macroporous silicon have been undertaken in Refs. 1–7. Due to the high aspect ratio this material is considered to be a good model structure for investigation of 2D PCs. Initially the samples for optical investigations were prepared either by cutting off from macroporous sample[1–3] or fabricated by a special 3D technique.[4–7] A characteristic feature of thus obtained structures was a strongly scattered surface that hindered optical measurements. Later on, the technology of simultaneous electrochemical etching of macropores and trenches (TP-technology) has been introduced.[8,9] This technology allows fabrication of narrow PC bars terminated with vertical Si side-walls. TP-technology of simultaneous etching of trenches and pores was investigated in details in Ref. 10. The conditions for fabrication of the smoothest side-walls and the minimal distortion of the pore shape were found in that work. A specific feature of the structures fabricated by TP-technology is the presence of the so-called pre-layer, i.e. a homogenous silicon layer which is a transition layer between air and photonic crystal structure. In Ref. 8 this layer was named as anti-refection layer (ARL), though the authors note that it is not actually antireflective in the common sense of this term. The pre-layer violates periodicity and can affect the reflection/transmission spectra of the PC bars.

The purpose of the present work is to calculate the reflection spectra of 2D PCs with finite width and a pre-layer using the scattering matrix method and the comparison of the simulated spectra with the experimental ones, registered with Fourier Transform Infrared (FTIR) micro-spectrometer.

Further author information: (Send correspondence to T.S.P.)
T.S.P.: E-mail: perovat@tcd.ie, Telephone: +353 1 896 14 32

Silicon Photonics VI, edited by Joel A. Kubby, Graham T. Reed, Proc. of SPIE Vol. 7943, 79431I · © 2011 SPIE · CCC code: 0277-786X/11/$18 · doi: 10.1117/12.882369

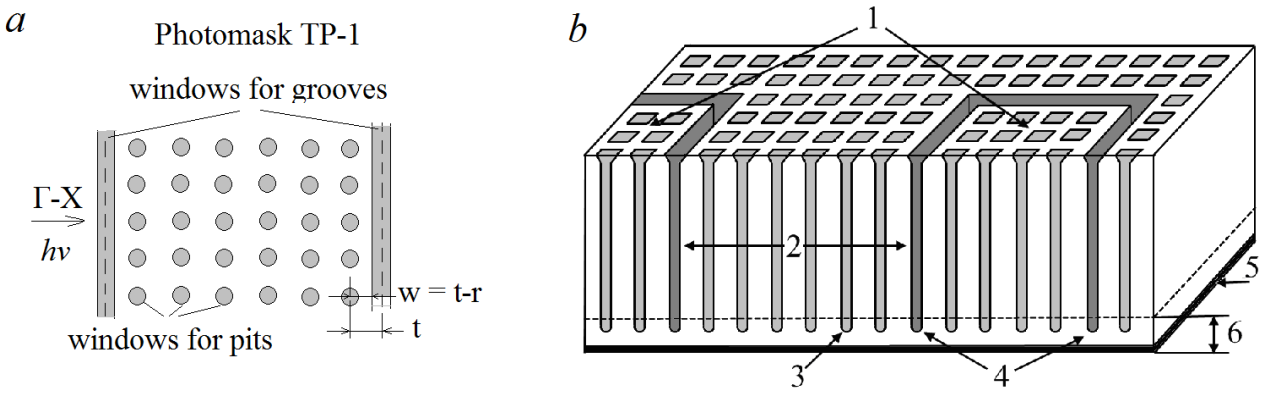

Figure 1. Schematic of the PC structure fabrication: a) the mask fragment for pits and grooves patterning, b) sample after PECE (1 — rectangular regions for elimination, 2 — PC bar, 3 — macropores, 4 — grooves; 5 — n^+ layer and 6 — the substrate eliminated during pores and grooves opening).

2. EXPERIMENTAL

To fabricate a square lattice of macropores in silicon wafer we used a photoelectrochemical etching (PECE) technique.[11,12] The process involves opening of windows in the oxide mask on the front surface of n-Si (100) by means of photolithography, alkaline etching of pits through the mask, and anodization in an HF solution under illumination from the back side of the wafer. To form PC bars of limited number of periods, pits and grooves were pre-patterned on the substrate surface simultaneously. The photomask schematic is shown in Fig. 1a. The pits and grooves served as nucleation centers for etching of deep macropores and trenches with the pore depth of $\sim 200\mu$m. The trenches define the rectangular areas of sample (see Fig. 1b) which can be eliminated after removal of the substrate by mechanical or chemical treatment. The resulted PC bars consist of 6 or 21 pore rows terminated with non-modulated silicon pre-layers (Fig. 2).

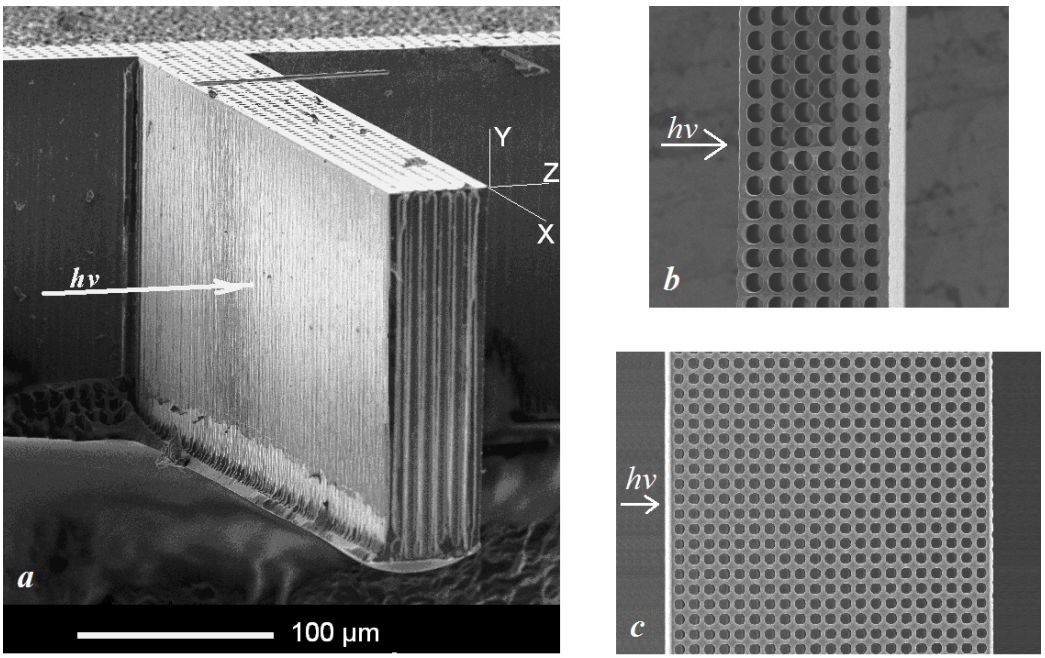

Figure 2. SEM images of the PC bars: a) cleaved structure; back-side view of the chips: b) with 6 pore rows (chip16-1) and c) with 21 rows (chip 16-2).

Table 1. Parameters of the PC bars.

Sample	Current density, j/j_{PS}	Depth of through pores, μm	Chip №	Number of pore rows	t, μm	Pore radius, r, μm
16.04.09N	0.35	155	16-1	6	10	2.5
			16-2	21	10	2.33

The photomask is characterized by two geometrical parameters, namely the lattice period, a, and the distance between trench center line and the centers of the adjacent pore row, t (see Fig. 1a). The etching process leads to the formation of air cylindrical pores of radius r and trenches of width $2r$. The pore radius and the trench width depend on the etching current density j and a subsequent treatment. The thickness of the pre-layer at the air-PC interface, w, depends on the difference between parameters t and r as $w = t - r$. In the present work we used the photomask with a=8 μm. The sample was etched in 4% HF in illumination-radius mode under initial current density value $j = 0.35 j_{PS}$, where j_{PS} is a critical current density that corresponds to the transition from pore formation mode to electro-polishing. The illumination-radius mode assumes a decrease of the current with time under PECE to maintain the pore radius unchanged within the depth. To remove the substrate we used either mechanical polishing (chip 16-1) or alkaline etching of the oxidized sample (chip 16-2). The value of the pore radius was found from the back-side image of the chips. Parameters of the samples are listed in Table 1.

3. FTIR MEASUREMENTS

Polarized FTIR measurements were performed in the range of 650-6500 cm^{-1} with a resolution of 8 cm^{-1} using a Digilab FTS 6000 spectrometer in conjunction with a UMA 500 infrared microscope. Gold coated glass slide was used as a 100% reflection reference. The rectangular aperture of 50×200 $\mu\mathrm{m}^2$ of the IR beam was used to provide a reasonable signal to noise ratio. A polarizer was placed in front of the microscope MCT detector. We use the notation for TE-polarization if the electric vector of the incident light is oriented perpendicular to the macropore channels (along the X-axis in Fig. 2a) and TM polarization if the electric vector is parallel to the macropore channels (along the Y-axis in Fig. 2a). As the incident light beam is focused on the sample as a cone between 10° and 30°, the average incident angle of 20° was used in calculations (see Ref. 2 for details).

4. RESULTS AND DISCUSSION

The reflection and transmission spectra, registered for two orthogonal polarizations of light for chip 16-1, are shown in Fig. 3. The transmission values are magnified by factors of 3 and 2.5 for TE and TM polarisations, respectively, for convenience of comparison of reflection and transmission spectra. As follows from the PC period, the first (lower) photonic band gap is located in the longer wavelength region than that accessible by our FTIR instrument. The experimentally investigated spectra are in the range of wavenumbers that correspond to the band gaps of high order. It can be seen from Fig. 3 that the maxima of the reflection spectra correspond to the minima of the transmission spectra and vice versa. The average value of the reflection coefficient is ∼0.5 and of the transmission coefficient is ∼0.1. The amplitude of modulation of the reflection spectra decreases from 0.55 to 0.15 as the wavenumber changes from 650 to 2500 cm^{-1}, while for the transmission coefficient it decays from 0.17 to 0.02 in the same spectral range. The increase of the number of periods from 6 to 21 in PC structure leads to the decrease in the intensity of the transmitted light up to ∼3-6 times depending on the wavelength. This type of behaviour is a characteristic feature of the spectra in the presence of diffuse scattering.[13]

Let us consider in more detail the calculation of the reflection spectra of the investigated structures. Different theoretical methods were developed for the modeling of light propagation in a photonic crystal. These methods have some advantages and disadvantages for application to different photonic structures. In particular, the plane wave expansion method is characterized by its poor convergence,[14] while the spherical-wave expansion method can be applied only for those PCs that composed of dielectric spheres and cylinders.[15,16] The Transfer Matrix Method (TMM)[17–20] is applicable for any periodic structures, however, it is not suitable for modeling of the structures with thick absorbing layers, due to a problem with mixing of the large and small numbers in the

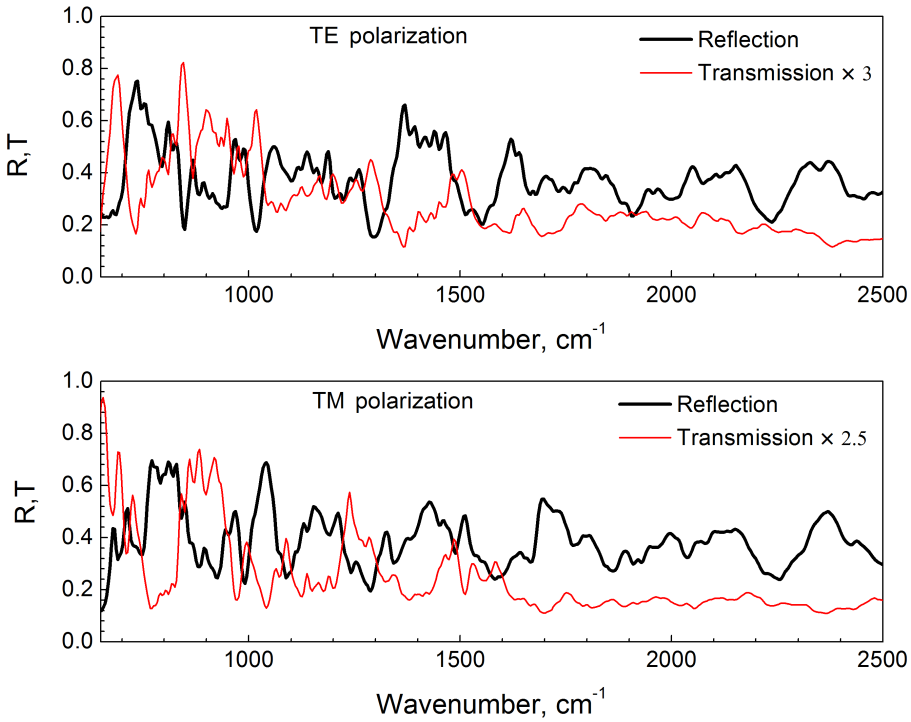

Figure 3. Experimental reflection and transmission spectra for TE and TM polarizations of sample 16-1.

transfer matrix.[21,22] The Finite-Difference Time Domain (FDTD) method[14,23] is the most common one, but it is very time-consuming. In the present work, we use the scattering matrix method (SMM). This method was proved to be very efficient for the investigation of dielectric and semiconductor layers with a finite number of lattice periods.[24,25]

The scattering matrix formalism[21,22] is a powerful tool for investigation of the eigenmodes of thin one- and two dimensionally periodic photonic crystal slabs.[24–27] The main idea of this method is to split the PC structure into several planar periodical layers and to find solution of the Maxwell equation in each layer by means of the expansion of the electric and magnetic fields into the Floquet-Fourier modes. The exact solution can be represented as an infinite series of these modes. In order to realize SMM numerically we have to take into account only first N_g elements. Then the solutions for all the layers must be connected to each other via the boundary conditions and the scattering matrix formalism. The calculation accuracy increases with increasing the number of used plane waves N_g, however the calculation time becomes longer. Nevertheless, for calculations of PCs, fabricated as alternating layers of dielectric and semiconductor components with relatively small number of periods, the calculations can be performed within a reasonable time scale.

In the present work we investigate the photonic crystal structures with a limited number of periods. As was mentioned above, in the experimental setup the focused incident light is used. Thus the light propagates along both Γ-X and Γ-M photonic crystal directions. A possible model structure consists of a number of periodical layers homogeneous along Z-axis as shown in Fig. 4. Figure 4 represents an example of 2D macroporous Si structure where each air cylinder is approximated by 30 modulated layers, so that the square lattice of the photonic crystal bar is modeled by 189 layers as a whole. The scattering matrix of this system of layers was constructed using the procedure described in Ref. 22. The scattering matrix of the entire structure was utilized for calculation of Z-components of the Pointing vectors for incoming and reflected light waves and the reflection coefficients. In the present work 29 plane waves were used. The average value of incident angle of 20° with respect to Z-axis (see Fig. 2a) was used as a direction of light propagation for spectra simulation by SMM.

The experimental and calculated reflection spectra for TE and TM polarizations are shown in Fig. 5 for sample 16-1. It can be seen from Fig. 5, that the 1-st (fundamental) photonic band gap is centered at $\sim$250 cm^{-1}

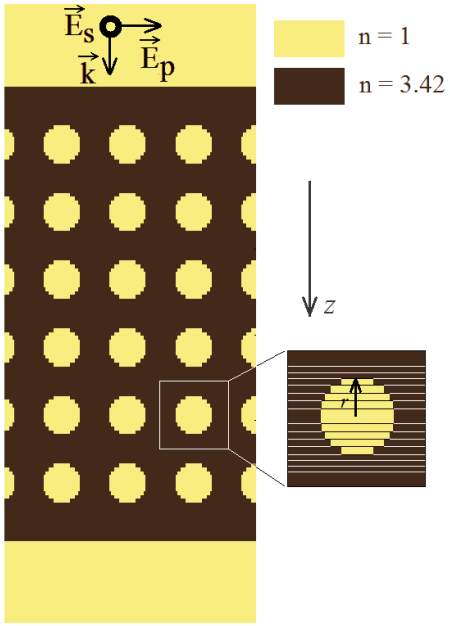

Figure 4. The ideal model of the photonic structure as a sequence of multilayers, homogeneous along Z-axis.

which is in agreement with results of Ref. 1. This particular range of spectra is outside of the experimentally available range. The calculated and experimental reflection spectra disagree in the whole investigated spectral range between 700 and 2500 cm^{-1}. The calculated reflection spectra are characterized by frequent oscillations of the reflection coefficient with the amplitude close to 1. The reason for this discrepancy can be the Rayleigh scattering of light on the irregularities of the PC structure, roughness of the inner surface of the air pores and

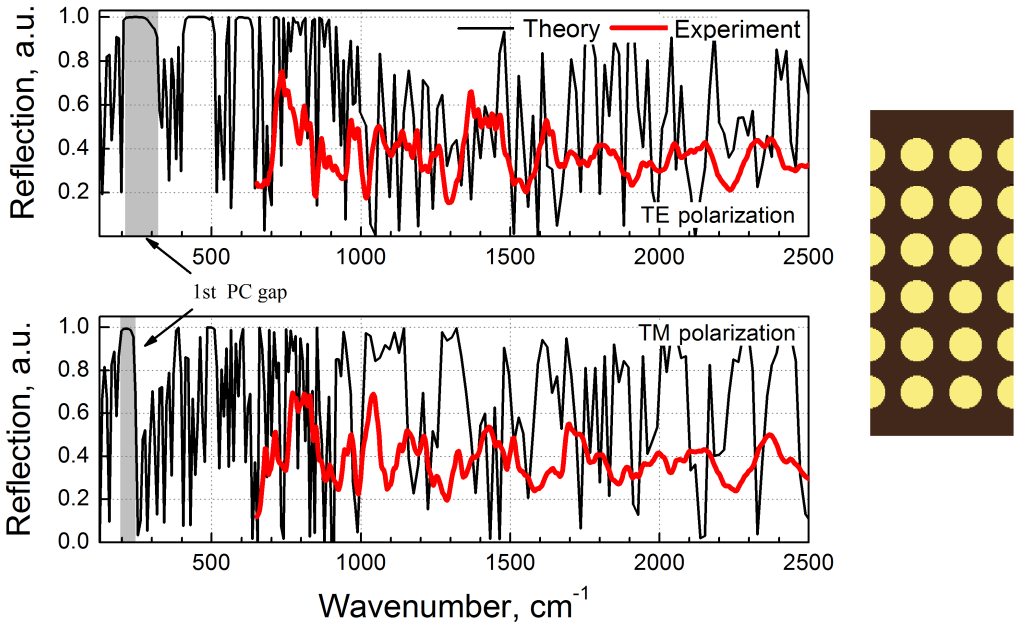

Figure 5. Experimental (thick line) and calculated with an ideal model (thin line) reflection spectra of the sample 16-1 (pore radius r =2.75 μm). Grey regions denote the 1-st photonic stop-band.

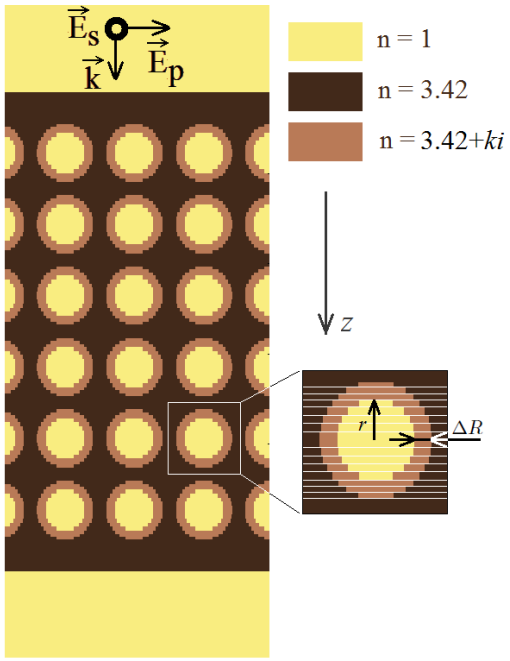

Figure 6. Three-component model for the photonic structure with scattering (absorbing) ring around the pores.

the interface between the photonic crystal bar and the incoming and outgoing media. This scattering can be essential because the investigated structures are characterized by a high optical contrast. It is known that the surface roughness affects the ellipsometry measurements,[17] for example. The deviation of the results in this case can be described by the Rayleigh scattering of light on the surface and interface roughness and, as a consequence, by losses in light propagation. There are a number of publications[28–31] where these losses of light are successfully taken into account by introduction of an imaginary part to the refractive indices of transparent materials.

In this work, for the accounting of light scattering a three-component model of PC structure was introduced with a nonzero absorption coefficient for silicon in the regions around pores as shown in Fig. 6. From now on two additional parameters which characterize the structure are introduced. These parameters are: the imaginary part of the refractive index of silicon in the ring around a pore, k, and the width of the ring of roughness around the pore, ΔR. During the fitting of the experimental reflection spectra shown in Fig. 3, we consider for simplicity that these parameters are not dependent on the wavelength of the incident light. Parameters k and ΔR were varied in the range from 0 to 1 and from 0 to 2 μm, accordingly, while the pore radius was varied in the range from 2.5 to 3.15 μm. The best agreement between the experimental and the theoretical spectra is obtained for r=2.75 μm, ΔR=0.8 μm and k=0.2 (see Fig. 7). Similar procedure was used for the fitting of the reflection spectra of chip 16-2, consisting of 21 periods (see Fig. 8).

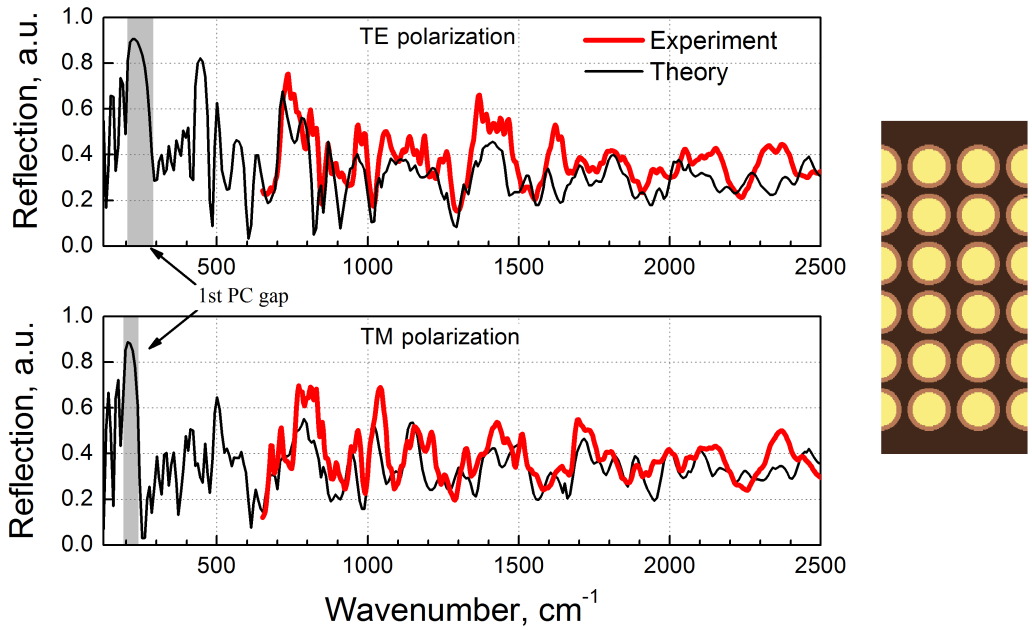

Figure 7. Experimental (thick line) and calculated with three-component model (thin line) reflection spectra for TE (top panel) and TM (bottom panel) polarizations of sample 16-1 (pore radius r=2.75 μm, ΔR=0.8 μm and κ=0.2). Grey regions denote the 1-st photonic stop-band.

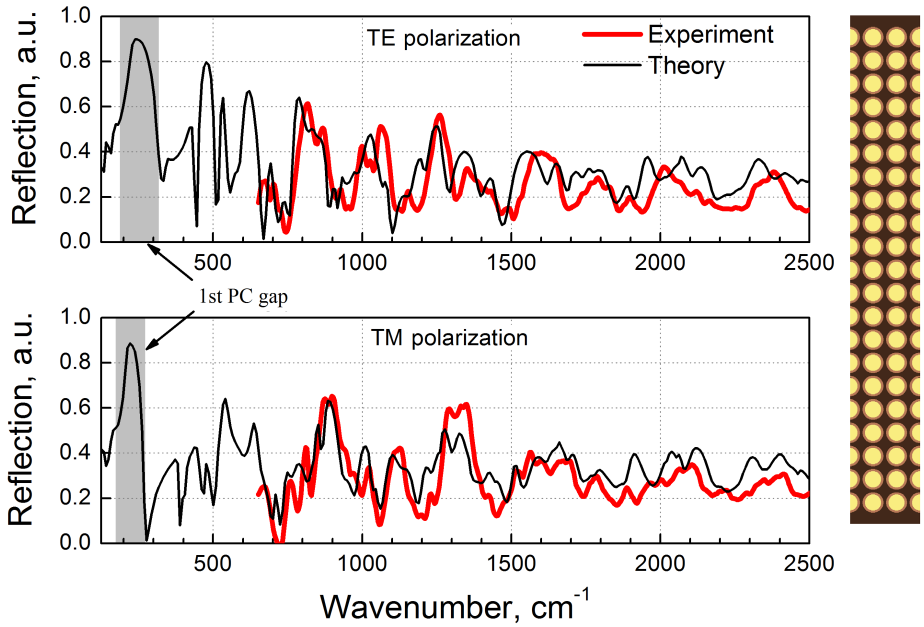

Figure 8. Experimental (thick line) and calculated with a 3-component model (thin line) reflection spectra for TE (top panel) and TM (bottom panel) polarizations of sample 16-2 (pore radius r=3 μm, ΔR=0.8 μm and κ=0.2). Grey regions denote the 1-st photonic stop-band.

It is interesting to compare the reflection spectra, calculated for the case of an ideal model and for the three-component model of the PC bar. As is seen from Fig. 9, TE- and TM-spectra obtained with three-component model have the first photonic band gap practically at the same wavenumbers, while the absolute value of the reflection coefficient and the bandwidth decreases. In the high-wavenumber range the spectra transformations are more dramatic: not only the strong oscillations are smoothened, but also the form of the spectra is changed significantly for both polarizations.

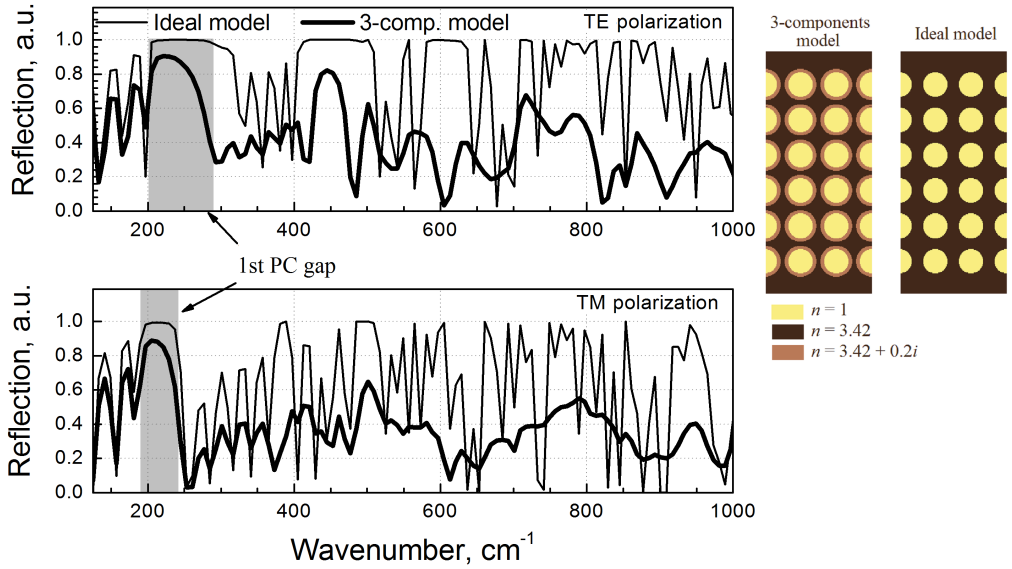

Figure 9. A comparison of reflection spectra calculated by an ideal model (thin line) and a 3-component model (thick line) for sample 16-1.

The specific feature of photonic crystal with the square lattice is the fact that photonic band gaps for all directions in the crystal do not overlap for TE and TM polarizations, so no complete band gaps can be obtained.[14,32] This fact does not contradict to our results, as we see overlapping of the band gaps just for a single Γ-X direction in the investigated PC structure.

5. CONCLUSION

The scattering matrix method was used for simulation of light propagation through the fabricated structures of macroporous Si two-dimensional photonic crystal with square lattice of deep cylindrical pores. Three-component model of the PC bar with the pre-layer was chosen as a model structure for the calculation of the reflection spectra by scattering matrix method. This model enables us to take into account the light scattering on the roughness of the inner surface of the air pores by introduction of the extinction coefficient of Si in a thin ring around a pore. It has been shown that spectra simulated according to this model are in a satisfactory agreement with the experiment.

ACKNOWLEDGMENTS

The study was financially supported by the Russian Foundation for Basic Research (project № 09-02-00782) and grant for support of leading scientific schools (NSh-3306-2010.2). S. A. Dyakov acknowledges IRCSET for financial support. Authors thank L. M. Portsel for useful discussion.

REFERENCES

[1] Gruning, U., Lehmann, V., and Engelhardt, C. M., "Two-dimensional infrared photonic band gap structure based on porous silicon," *Appl. Phys. Lett.* **66**(24), 2329 (1995).

[2] Rowson, S., Chelnokov, A., Cuisin, C., and Louritoz, J.-M., "Two-dimensional photonic bandgap reflectors for free-propagating beams in the mid-infrared," *J. Opt. A: Pure Appl. Opt.* **1**(4), 483–489 (1999).

[3] Rowson, S., Chelnokov, A., Louritoz, J.-M., and Carcenac, F., "Reflection and transmission characterization of a hexagonal photonic crystal in the mid infrared," *J. Appl. Phys.* **83**(10), 5061–5064 (1998).

[4] Ottow, S., Lehmann, V., and Föll, H., "Processing of three-dimensional microstructures using macroporous n-type silicon," *J.Electrochem. Soc.* **143**(1), 385–390 (1996).

[5] Schilling, J., Birner, A., Müller, F., Wehrspohn, R. B., Hillebrand, R., Gösele, U., Busch, K., Johnc, S., Leonardc, S. W., and van Drielc, H. M., "Optical characterisation of 2d macroporous silicon photonic crystals with bandgaps around 3.5 and 1.3 μm," *Opt. Mat.* **17**(1), 7–10 (2001).

[6] Jamois, C., Wehrspohn, R. B., Andreani, L. C., Hermann, C., Hess, O., and Gösele, U., "Silicon-based two-dimensional photonic crystal waveguides," *Photonics and Nanostructures — Fundamentals and Applications* **1**(1), 1–13 (2001).

[7] Busch, K., Lölkes, S., R.Wehrspohn, and Föll, R., [*Photonic Crystals. Advances in Design. Fabrication, and Characterization*], Weinheim: Wiley-VCH (2004).

[8] Geppert, T., Schweizer, S. L., U.Gösele, and Wehrspohn, R. B., "Deep trench etching in macroporous silicon," *Appl. Phys. A* **84**(3), 237–242 (2006).

[9] Wehrspohn, R. B., Schweizer, S. L., and Sandoghdar, V., "Linear and non-linear optical experiments based on macroporous silicon photonic crystals," *Phys. Stat. Sol. A* **204**(11), 3708–3726 (2007).

[10] Astrova, E. V., Fedulova, G. V., and Guschina, E. V., "Formation of 2d photonic crystal bars by simultaneous photoelectrochemical etching of trenches and macropores in silicon," *Semiconductors* **44**(12), 1617–1623 (2010).

[11] Lehmann, V. and Föll, H., "Formation mechanism and properties of electrochemically etched trenches in n-type silicon," *J. Electrochem. Soc.* **137**(2), 653–659 (1990).

[12] Lehmann, V., [*Electrochemistry of Silicon*], Wiley-VCH, D-69469 Weinheim (2002).

[13] Astrova, E. V., Tolmachev, V. A., Fedulova, G. V., Melnikov, V. A., Ankudinov, A. V., and Perova, T. S., "Optical properties of one-dimensional photonic crystals fabricated by photo-electrochemical etching of silicon," *Appl. Phys. A* **98**(3), 571–581 (2010).

[14] Sakoda, K., [*Optical Properties of Photonic Crystals*], Springer (2001).

[15] Ohtaka, K., "Energy band of photons and low-energy photon diffraction," *Phys. Rev. B* **19**(10), 5057–5067 (1979).
[16] Stefanou, N., Karathanos, V., and Modinos, A., "Scattering of electromagnetic waves by periodic structures," *J. Phys.: Condens. Matter* **4**(36), 7389–7400 (1992).
[17] Azzam, R. M. A. and Bashara, N. M., [*Ellipsometry and Polarized Light*], North-Holland Personal Libriary (1987).
[18] Brand, S. and Hughes, D. T., "Calculations of bound states in the valence band of AlAs/GaAs/AlAs and AlGaAs/GaAs/AlGaAs quantum wells," *Semicond. Sci. Technol* **2**(9), 607–614 (1987).
[19] Mailhoit, C. and Smith, D. L., "$k-p$ theory of semiconductor superlattice electronic structure," *Phys. Rev. B* **33**(12), 8360–8372 (1986).
[20] Pendry, J. B. and MacKinnon, A., "Calculation of photon dispersion relations," *Phys. Rev. Lett.* **69**(19), 2772–2775 (1992).
[21] Whittaker, D. M. and Culshaw, I. S., "Scattering-matrix treatment of patterned multilayer photonic structures," *Phys. Rev. B* **60**(24), 2610–2618 (1999).
[22] Tikhodeev, S. G., Yablonskii, A. L., Muljarov, E. A., Gippius, N. A., and Ishihara, T., "Quasiguided modes and optical properties of photonic crystal slabs," *Phys. Rev. B* **66**, 045102 (2002).
[23] Taflove, A., [*Computational Electrodinamics: The Finite-Difference Time-Domain Method*], Artech House, Boston (1995).
[24] Gippius, N. A., Tikhodeev, S. G., and Ishihara, T., "Optical properties of photonic crystal slabs with an asymmetrical unit cell," *Phys. Rev. B* **72**(4), 045138 (2005).
[25] Christ, A., Tikhodeev, S. G., Gippius, N. A., Kuhl, J., and Giessen, H., "Waveguide-plasmon polaritons: Strong coupling of photonic and electronic resonances in a metallic photonic crystal slab," *Phys. Rev. Lett.* **91**(18), 183901 (2003).
[26] Gippius, N. A. and Tikhodeev, S. G., "Application of the scattering matrix method for calculating the optical properties of metamaterials," *Phys.-Usp.* **52**(9), 967–971 (2009).
[27] Gippius, N. A., Weiss, T., Tikhodeev, S. G., and Giessen, H., "Resonant mode coupling of optical resonances in stacked nanostructures," *Optics Express* **18**(7), 7569–7574 (2010).
[28] Azzam, R. M. A. and Bashara, N. M., "Polarization characteristics of scattered radiation from a diffraction grating by ellipsometry with application to surface roughness," *Phys. Rev. B* **5**(12), 4721–4729 (1972).
[29] Maradudin, A. A. and Mills, D. L., "Scattering and absorption of electromagnetic radiation by a semi-infinite medium in the presence of surface roughness," *Phys. Rev. B* **11**(4), 1392–1415 (1975).
[30] Benisty, H., Labilloy, D., Weisbuch, C., Smith, C. J. M., Krauss, T. F., Cassagne, D., Béraud, A., , and Jouanin, C., "Radiation losses of waveguide-based two-dimensional photonic crystals: Positive role of the substrate," *Appl. Phys. Lett.* **76**(5), 532–534 (2000).
[31] Benisty, H., Lalanne, P., Olivier, S., Rattier, M., Weisbuch, C., Smith, C. J. M., Krauss, T. F., Jouanin, C., and Cassagne, D., "Finite-depth and intrinsic losses in vertically etched two-dimensional photonic crystals," *Opt. Quantum Electronics* **34**(1), 205–215 (2002).
[32] Joannopoulos, J. D., Meade, R. D., and Winn, J. N., [*Photonic crystals: Molding the flow of light*], Prinston University Press, Chichester, West Sussex (1995).